Proceedings of The National Conference
On Undergraduate Research (NCUR) 2013
University of Wisconsin La Crosse, WI
April 11-13, 2013

Design of a Scaled-Up Experiment to Study an Impinging Synthetic Jet

Isaac Rose
Mechanical Engineering
Villanova University
Villanova, PA 19085

Faculty Advisor: Dr. Alfonso Ortega

Abstract

A jet can be synthesized by forcing fluid into and out of an orifice or channel in rapid succession. Even though synthetic jets introduce no net mass flow into a system, they deliver flow with net positive momentum as they generate a train of vortex pairs that self-sustain an outward periodic flow. Consequently, this technique can be potentially employed to remove heat in confined spaces, such as small scale electronics, as the flow can be actuated utilizing relatively small piezoelectric devices. The present work reports on the design of laboratory experiments that can replicate prior numerical investigations of a synthetic jet impinging normal onto a heated surface. The Reynolds and Womersley numbers were used to geometrically scale up the experiment from a small scale to a larger, more practical size. The intention of the latter was to allow highly resolved measurements of the unsteady velocity field and the local time-averaged Nusselt number on the target heated surface. Data were collected for various Reynolds numbers, driver frequencies, and jet-to-surface distances, and subsequently compared to computational results. Good to marginal agreement was found between numerical and empirical results. It is hypothesized that lateral heat losses that occurred in the substrate become comparable in magnitude to the convected heat, therefore contaminating the data. Moreover, when the jet channel is placed at a larger distance from the heated surface, the fluid flow transitions from laminar to turbulent and may undergo three-dimensional effects as well. These phenomena were not allowed in the idealized computations.

Keywords: Synthetic Jet, convective heat transfer, impingement

1. Introduction

A synthetic Jet is a device which consists of an orifice, a cavity, and an oscillating membrane. Fluid is cyclically ejected and injected out of the orifice. Vortices are formed during the ejection of fluid which continue to travel away from the jet exit even while the injection of fluid is occurring. For each full cycle of the membrane one set of vortices is created (the orientation of these vortices depends on the geometry of the orifice).

This type of flow is advantageous for use as a cooling mechanism in comparison to conventional steady jets. The vortices cause mixing of fluid to occur which entrains cooler fluid closer to a heated surface, cooling it more effectively. Piezoelectric materials have been used to make small synthetic jets for cooling electronic components like LEDs or computer chips. These materials change shape when current is applied to them. By applying a sinusoidal electrical signal to the devices, an oscillatory motion of the piezoelectric membrane results which is used to displace the fluid required for the synthetic jet. An added benefit of these devices is that they can operate at low decibel levels compared to conventional fans. A large part of the research conducted has been performed with the ultimate goal of determining the relative efficiency of synthetic jets compared to steady jets in order to fully understand these advantages.

Smith and Glezer[1] studied the formation of vortices created by a synthetic jet with a rectangular slot. They concluded that two counter rotating vortices are formed during each ejection of fluid, and that during the following injection period the previously created vortices are only slightly affected.

Smith and Swift[2] compared synthetic and steady jets. They found experimentally that flow produced by synthetic jets is slower and wider than that produced by steady jets. They also found that fluid flow produced by synthetic jets transitions to turbulent flow at lower Reynolds numbers than that produced by steady jets.

Other research has been done on the cooling capabilities of synthetic jets[3-16]. Gillespie et al[3] found that the highest heat transfer rates for an impinging synthetic were at intermediate jet-to-surface distances, about $7<z/S<18$. Where z is the jet-to-surface distance and S is the nozzle width. The effect of jet driving frequency and Reynolds number on heat transfer rates for a round jet was studied by Pavlova and Amitay[6]. They concluded that at high frequencies close spacing was advantageous, and the opposite was true for low frequencies. Multiple researchers have studied the effect of matching the driving frequency with the resonant frequency of the cavity[3,5-7] and found that exit velocities increase when a synthetic jet is produced under these conditions. Numerical computations of fluid velocity at the nozzle exit[11,17] have shown that it is accurate to assume laminar flow and a sine wave velocity function.

2. Motivation

While some research on the cooling capabilities of synthetic jets has been performed, there is a lack of fundamental understanding of the fluid dynamics and heat transfer phenomena taking place. Specifically, the effects of varying the driving frequency while keeping the Reynolds number constant, and vice versa, on the heat transfer rates have not been addressed. Additionally, the de-coupling of the fluid flow of a synthetic jet from the way in which the flow is produced in order to minimize artifact effects has not been considered. Therefore, our intention is to create an experiment to eliminate, or at least minimize, these effects.

3. Problem Description

The commercial software ANSYS FLUENT™ was used to perform numerical experiments on a canonical synthetic jet impinging over a heated surface. The simulations were used to predict the heat transfer rates along the heated surface for varying conditions.

The simulation was based on the assumptions that: the fluid flowed between two adiabatic inviscid parallel plates which were separated by a distance (w) of 1mm, the flow was two dimensional and laminar, and the velocity followed a sinusoidal function with respect to time.

Experimental data are needed to verify the validity of the results of this simulation. In order to obtain data that are comparable to the numerical simulations, a physical model must be constructed that resembles the idealized geometry as close as possible.

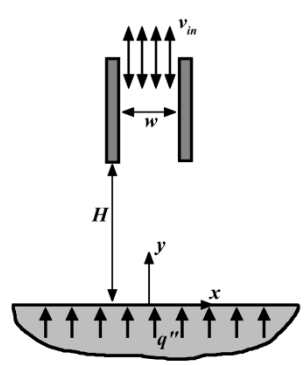

Figure 1. Schematic of the physical domain that represents the canonical geometry

4. Solution Procedure

The parameters that drive the heat transfer and fluid dynamic phenomena are the Reynolds number and the Womersley number. They are defined as follows:

$$Re = \frac{U_0 w}{v} \tag{1}$$

$$U_0 = L_0 f \tag{2}$$

$$L_0 = \frac{1}{w}\int_0^{T/2}\int_0^{w} u(x,t)dxdt \tag{3}$$

$$u(x,t) = u_{max}(x)\sin(2\pi f t) \tag{4}$$

$$\Omega = \sqrt{\frac{2\pi f w^2}{v}} \tag{5}$$

Where Re=Reynolds number, U_0 is the characteristic velocity, w is the nozzle width, v is the fluid viscosity, L_0 is the characteristic length, f is the driving frequency, $u(x,t)$ is the fluid velocity at the nozzle exit as a function of position and time, $u_{max}(x)$ is the maximum fluid velocity with respect to position, and Ω is the Womersley number.

The fluid velocity at the jet exit follows a sinusoidal curve[17]. By taking the integral of the fluid velocity at the jet exit during the blowing part of one cycle, the stroke length, L_0, can be found. This quantity is proportional to the volume of fluid exiting the nozzle. The characteristic velocity is defined in terms of the stroke length and the frequency. Equation (1) is generally accepted in literature and has been used successfully to compare continuous and synthetic jets[1,2].

A scaled-up experiment was designed by keeping these dominant non-dimensional numbers the same as those in the numerical simulation. This ensures that the flow characteristics remain equal. These two non-dimensional parameters were calculated for the varying fluid velocities and frequencies used in the numerical simulation. Then the corresponding velocities and frequencies were found for a physical experiment that was six times larger than the numerical model (nozzle width is 6mm instead of 1mm).

Table 1. comparison of numerical and corresponding experimental Reynolds and Womersley numbers

Reynolds Number	305	407	508	Womersley Number	12.66	17.9	21.93
umax numerical	15	20	25	f numerical	400	800	1200
umax experimental	2.5	3.333	4.167	f experimental	11.11	22.22	33.33

(Velocities in m/s frequencies in Hz)

A sub-woofer type of acoustic speaker was used to produce the desired frequencies. The resulting fluid velocity at the jet exit produced by the speaker oscillations had to be externally determined. It was also necessary to verify that the speaker driver oscillated with a consistent amplitude and frequency for a given sinusoidal output voltage sent from the compact DAQ to the amplifier, then to the speaker (see figure 2). The position of the speaker driver with respect to time was measured using a laser displacement sensor. The data obtained show that the driver does follow a consistent sinusoidal pattern for a given input signal (figure 3).

The speaker was connected to a wooden and aluminum assembly consisting of a plenum, converging channel, and nozzle. The nozzle was rectangular shaped and had a width of 6mm and aspect ratio of 50:1. The large ratio prevents three dimensional effects from occurring.

In order to calculate the Reynolds numbers it was necessary to know the fluid velocity at the nozzle exit with respect to time and position in the spanwise direction. A hot wire anemometer was used to take velocity

measurements at different positions along the nozzle exit as well as for different output voltage signals. The data were then curve fitted to find the sinusoidal function for velocity with respect to time for each output signal.

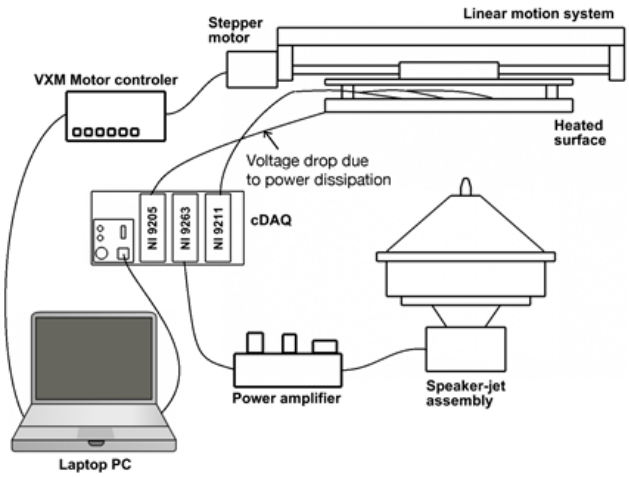

Figure 2. schematic of experiment assembly

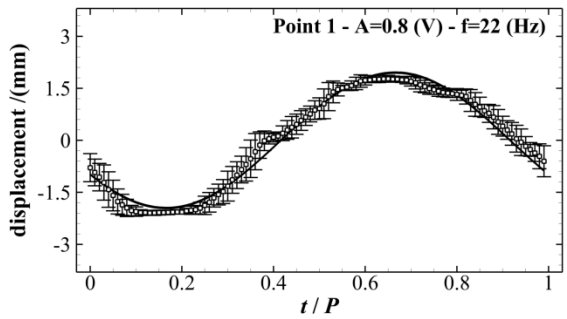

Figure 3. displacement of speaker cone during one cycle P=period (s)

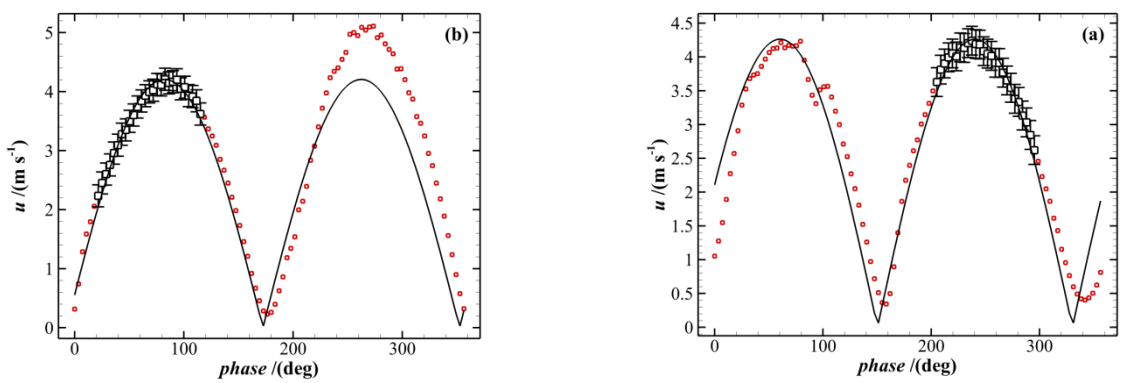

Figure 4. velocity measurements of the hot wire anemometer for (a) A=0.8 (V) f=11.11 (Hz) and (b) A=0.5 (V) f=33.33 (Hz) (A is the amplitude of the sinusoidal input signal)

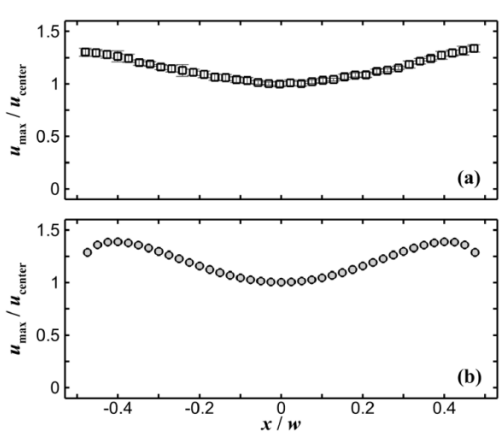

Figure 5. maximum fluid velocity measurements along the width of the nozzle (a) experimental data, (b) canonical

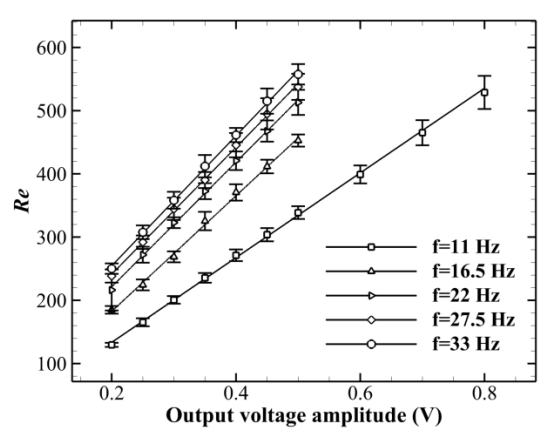

Figure 6. Reynolds number vs output voltage amplitude

Significant deviations are apparent for one half of each full cycle as shown in figure 4. This is most likely due to the fact that the anemometer distorted the fluid flow during the backstroke of the driver. For this reason only data points recorded during the forward stroke (black data points) were used when curve fitting.

The maximum velocity for each sinusoidal function was found. These data points represent the maximum fluid velocity at a given position along the nozzle width in the spanwise direction. The resulting data (figure 5 a) show good agreement with numerical predictions (figure 5 b). The velocity increases for both experimental and numerical data near the nozzle walls (x/w=-0.5 and 0.5). This is expected since the fluid tends to bifurcate as it leaves the nozzle and immediately forms a vortex pair. The increase in fluid velocity near the nozzle walls seen in the numerical prediction (Figure 5 b) with respect to the experimental data (figure 5 a) is due to the absence of fluid-to-wall shearing in the numerical simulation.

Integration of these discrete data points was done using Simpson's rule. All variables defining the Reynolds number were now known so it was possible to relate the Reynolds number to the output signal. This process was repeated several times for different signal frequencies and amplitudes. The following relationship between voltage amplitude, frequency and resulting Reynolds number was found (figure 6).

In order to determine the effect of each parameter on the heat transfer phenomena occurring, it is advantageous to be able to change only one parameter while keeping the others constant. Previous experimental work has yielded inconsistent data due, in a large part, to the fact that the Reynolds number was not kept constant while the driving frequency was changed. However, in this work the Reynolds number remained constant while the frequency was varied by changing the input voltage amplitude accordingly.

4.1 Heated Surface Design

The heated surface was designed to have a smooth top surface above the heater, decreasing the likelihood of flow disturbances, and a thermally insulating substrate below the heater. Balsa wood was used as the substrate because of its low thermal conductivity. This reduced heat loss due to conduction into the substrate. The balsa wood was fastened to a phenolic plate for increased structural integrity as shown in figure 7. The heater itself is made from electrically conductive traces which dissipate heat when voltage is applied. Three K-type thermocouples were placed along the centerline of the heater spaced evenly apart. A 0.001" thick stainless steel sheet was placed on top of the heater to smoothen any imperfections on the heater as well as possible small bumps created by the thermocouples.

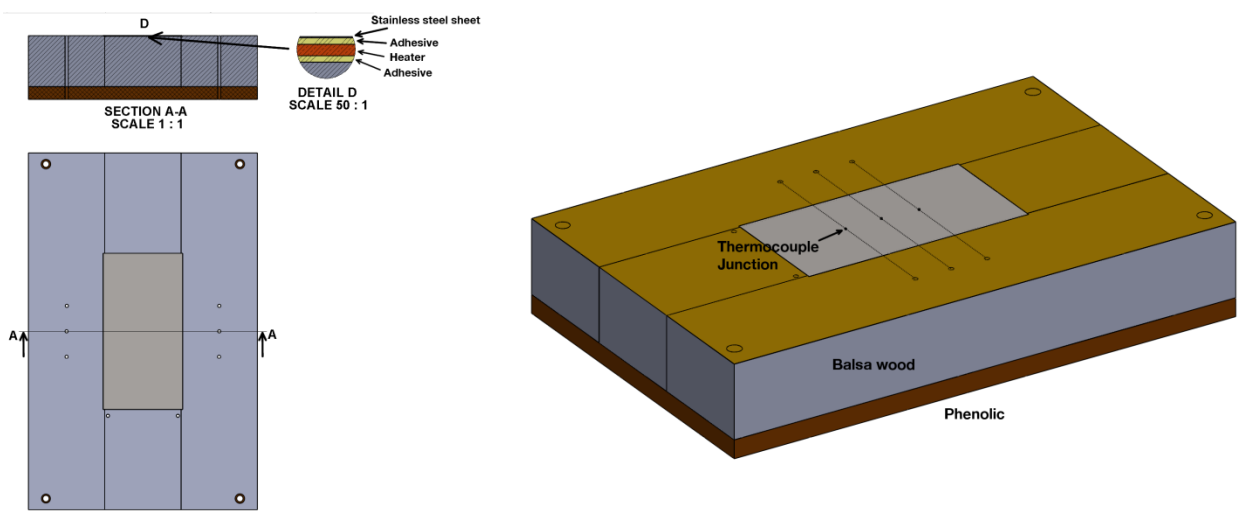

Figure 7. SolidWorks model of heated surface design

The surface was oriented facing downwards to reduce the effects of natural convection (see Figure 8). A separate structure was used to support the synthetic jet so that small vibrations caused by the oscillations of the speaker driver did not translate to the heated surface, affecting temperature measurements.

The three thermocouples were used to take temperature measurements along the heated surface. The surface was moved with respect to the nozzle in the spanwise direction to record the surface temperature over a wide spatial range and with good resolution (see figure 9).

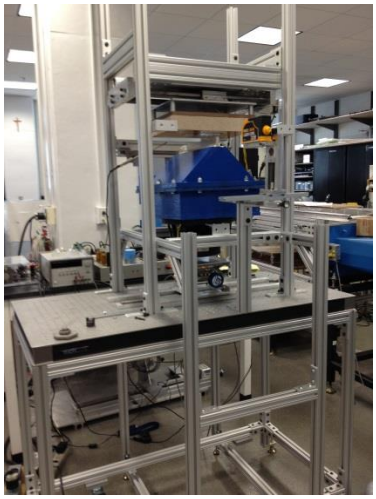

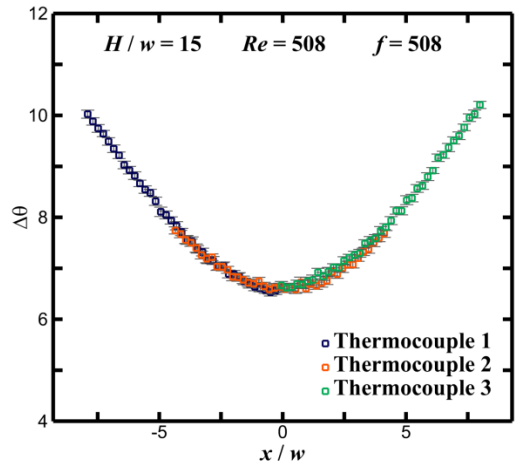

Figures 8 (left) and 9 (right). Left: Synthetic jet rig assembly, Right: Thermocouple measurements of temperature distribution on heated surface (Δθ=difference in temperature between surface and fluid exiting jet nozzle)

4.2 Estimation Of Heat Transfer

The time averaged Nusselt number distribution was calculated based on the temperature measurements taken at the surface and the known amount of power being dissipated by the heater. The dissipated power was found simply by using Joule's first law and Ohm's law. A known voltage was applied across the heater, and a shunt resistor of known resistance placed in parallel to the heater was used to calculate the current flowing through the circuit. The Nusselt number was calculated as follows:

$$Nu = \frac{hw}{k} \tag{6}$$

Where h is the heat transfer coefficient at the heated surface, w is the nozzle width, and k is the thermal conductivity of air. h was obtained by first taking an energy balance at the heated surface (Eq. (7)) then substituting Newton's law of cooling, Fourier's law, and the Stefan-Boltzmann law for q''_{conv}, q''_{cond} and q''_{rad} respectively.

$$q''_{heater} = q''_{conv} + q''_{cond} + q''_{rad} \tag{7}$$

Where q''_{heater} is the total heat dissipated by the heater. Rearranging and solving for h leads to the following.

$$h = \frac{q''_{heater}}{T_w - T_j} - \frac{1}{\frac{L_B}{k_B} + \frac{L_{ph}}{k_{ph}} + \frac{1}{h_{back}}} - \varepsilon\sigma(T_w + T_j)(T_w^2 + T_j^2) \tag{8}$$

Where T_w is the temperature of heated surface, T_j is the temperature of ambient air, L_B is the thickness of the balsa wood, $k_B$is the thermal conductivity of the balsa wood, L_{ph} is the thickness of the phenolic, k_{ph} is the thermal conductivity of the phenolic, h_{back} is the heat transfer coefficient on the back surface of the phenolic, ε is the emissivity of the heater, σ is the Stefa-Boltzmann constant.

5. Results

It was found by analyzing the data that the heat transfer rates at the experimental surface were consistent with those found in the numerical simulation, as well as other previously published canonical simulations[14] for High Re, and low Ω and H/w values. For lower Re, and for higher Ω and H/w values discrepancies become clearly evident (Figures 10 and 11)

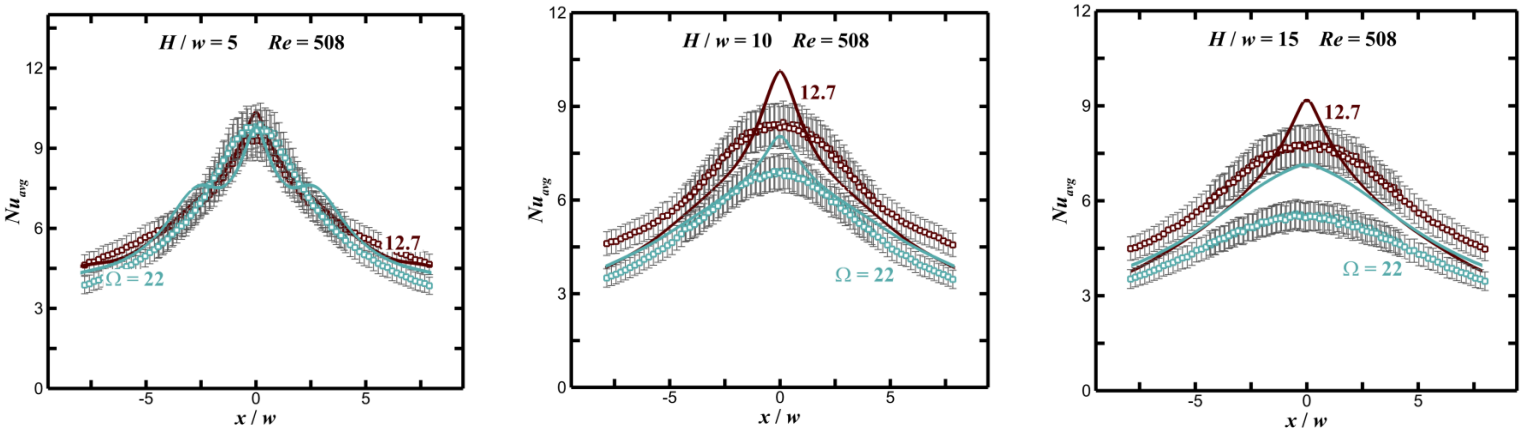

Figure 10. Time averaged Nusselt number at different operating conditions. Symbols=Experimental, Solid line= Numerical

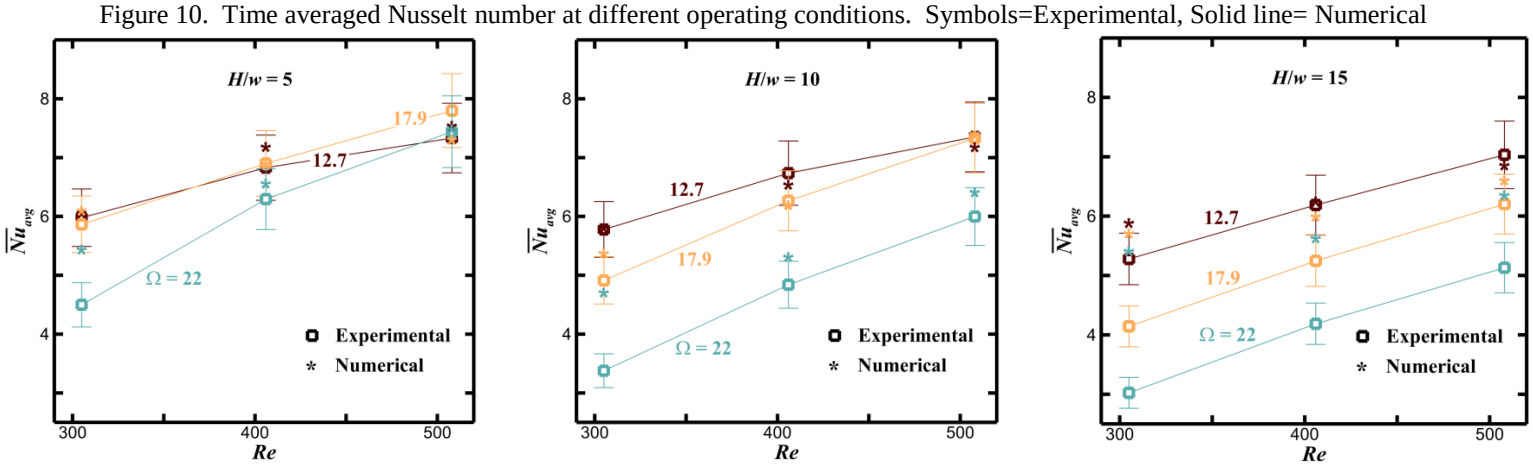

Figure 11. Space and time averaged Nusselt number vs Re for H/w= 5,10 and 15

As H/w increases and the Reynolds number decreases the experimental Nusselt number distribution becomes "flattened" with respect to the numerical prediction (figure 10). There are two probable causes of this "flattening". The first is the fact that the numerical simulation did not account for heat losses due to conduction through the substrate. It was assumed that all the heat produced by the surface was convected into the fluid in the numerical simulation, however this was not the case in the experiment. While the thermal conductivity of balsa wood is very low, it is not zero; therefore heat transfer into the substrate is inevitable. This increase in conductive heat losses would decrease the amount of convective heat loss which would decrease the Nusselt number overall. At larger jet-to-surface distances the conductive heat losses would increase since the fluid reaching the surface has less momentum resulting in a lower heat transfer coefficient.

The second is that at larger x/w distances the fluid flow tends to transition from laminar to turbulent[1]. The heat transfer coefficient for turbulent flow would be higher than that for laminar flow. The Nusselt number distribution of the numerical simulation would be lower than that of the experimental simulation at larger x/w distances because the numerical simulation did not account for turbulent fluid flow.

Another possible cause for discrepancies is the fact that three dimensional effects can appear. At larger H/w the vortices have more time to develop, and may lose their coherence and symmetry.

Positioning the heated surface facing downward mitigated the effects of natural convection. The ratio between natural and forced convection (Richardson number) was found to be between 0.047 and 0.26. Heat transfer due to natural convection becomes comparable to that due to forced convection when the Richardson number approaches unity. While the values found for the Richardson number were low, natural convection may still be significant when the flow arrives at the heated surface with low momentum.

6. Conclusion and Future Work

This empirical work shows the successful scaling up of prior idealized numerical simulations. However, significant deviations in results were present at large jet-to-surface distances, high frequencies, and low Reynolds numbers. Future work includes reconstructing the jet nozzle to have a smaller width. This will increase the heat transfer coefficient by increasing the fluid exit velocity which will render heat losses due to conduction insignificant.

7. References

1. Smith, B. L., and Glezer, A., "The formation and evolution of synthetic jets," Physics of Fluids, 10(9), 1998: 2281-2297.
2. Smith, B. L., and Swift, G. W., "A comparison between synthetic jets and continuous jets," Exp. Fluids, 34(4), 2003: 467-472.
3. Gillespie, M. B., Black, W. Z., Rinehart, C., and Glezer, A., "Local convective heat transfer from a constant heat flux flat plate cooled by synthetic air jets," Journal of Heat Transfer, 128(10), 2006: 990-1000.
4. Garg, J., Arik, M., Weaver, S., Wetzel, T., and Saddoughi, S., "Meso Scale Pulsating Jets for Electronics Cooling," Journal of Electronic Packaging, 127(4), 2005: 503-511.
5. Arik, M., "An investigation into feasibility of impingement heat transfer and acoustic abatement of meso scale synthetic jets," Appl. Therm. Eng., 27(8-9), 2007: 1483-1494. 10 Copyright © 2013 by ASME
6. Pavlova, A., and Amitay, M., "Electronic cooling using synthetic jet impingement," Journal of Heat Transfer-Transactions of the Asme, 128(9), 2006: 897-907.
7. Zhang, J. Z., and Tan, X. M., "Experimental study on flow and heat transfer characteristics of synthetic jet driven by piezoelectric actuator," Science in China Series E-Technological Sciences, 50(2), 2007: 221-229.
8. Arik, M., "Local heat transfer coefficients of a highfrequency synthetic jet during impingement cooling over flat surfaces," Heat Transfer Engineering, 29(9), 2008: 763- 773.
9. Valiorgue, P., Persoons, T., McGuinn, A., and Murray, D. B., "Heat transfer mechanisms in an impinging synthetic jet for a small jet-to-surface spacing," Experimental Thermal and Fluid Science, 33(4), 2009: 597- 603.
10. Chaudhari, M., Puranik, B., and Agrawal, A., "Heat transfer characteristics of synthetic jet impingement cooling," Int. J. Heat Mass Transf., 53(5-6), 2010: 1057- 1069.
11. Utturkar, Y., Arik, M., Seeley, C. E., and Gursoy, M., "An experimental and computational heat transfer study of pulsating jets," Journal of Heat Transfer- Transactions of the Asme, 130(6), 2008: 062201.
12. Jagannatha, D., Narayanaswamy, R., and Chandratilleke, T. T., "Analysis of a Synthetic Jet-Based Electronic Cooling Module," Numerical Heat Transfer Part a- Applications, 56(3), 2009: 211-229.
13. Chaudhari, M., Puranik, B., and Agrawal, A., "Effect of orifice shape in synthetic jet based impingement cooling," Experimental Thermal and Fluid Science, 34(2), 2010: 246-256.
14. Silva, L., and Ortega, A., 2010, "Convective Heat Transfer Due to an Impinging Synthetic Jet: A Numerical Investigation of a Canonical Geometry," Proc. 12th IEEE Intersociety Conference on Thermal and Thermomechanical Phenomena in Electric Systems, Omnipress.
15. Silva, L., and Ortega, A., 2011, "Numerical Simulation of Local Heat Transfer and Scaling of a Synthetic Impinging Jet in a Canonical Geometry," Proc. ASME 2011 Pacific Rim Technical Conference & Exposition on Packaging and Integration of Electronic and Photonic InterPACK.

16. Silva, L., and Ortega, A., 2011, "CFD Analysis of the Vortex Dynamics Generated by a Synthetic Jet Impinging on a Heated Surface," ASME 2011 International Mechanical Engineering Congress & ExpositionDenver, Colorado, USA.

17. Wang, Y., Yuan, G., Yoon, Y. K., Allen, M. G., and Bidstrup, S. A., "Large eddy simulation (LES) for synthetic jet thermal management," Int. J. Heat Mass Transf., 49(13-14), 2006: 2173-2179.